Transcrystallization in Fiber-Reinforced Isotactic Polypropylene Composites in a Temperature Gradient

YUQI CAI,[1] JÜRGEN PETERMANN,[1] HANS WITTICH[2]

[1] LS für Werkstoffkunde, FB Chemietechnik, Universität Dortmund, 44221-Dortmund, Germany

[2] AB Kunststoffe & Verbundwerkstoffe, Technische Universität Hamburg-Harburg, 21073-Hamburg, Germany

Received 27 June 1996; accepted 6 December 1996

ABSTRACT: Transcrystallization of isotactic polypropylene (iPP) on different fibers (carbon fiber, glass fiber, and aramid fiber) was conducted in a temperature gradient. The Ultra-High-Module carbon fiber (UHMCF), the High-Module carbon fiber, and the aramid fiber (Twaron) showed sufficient nucleation ability to form transcrystallization of iPP in certain temperature ranges. Among them, the UHMCF showed the best nucleation ability. On the contrary, the Intermediate-Module carbon fiber, the High-Tenacity carbon fiber, and the E-glass fiber showed too low nucleation ability to form transcrystallization of iPP. One efficient way to induce transcrystallization on these fibers was proved by pulling the fibers in supercooled iPP melts. The interface shear between fiber and supercooled matrix melt on crystallization and the interface temperature gradient between fiber and supercooled matrix melt on crystallization are considered to be two very important factors for the formation of transcrystallization. © 1997 John Wiley & Sons, Inc. J Appl Polym Sci **65:** 67–75, 1997

Key words: transcrystallization; nucleation; lamellae; interface shear; interface temperature gradient

INTRODUCTION

Fiber-reinforced semicrystalline thermoplastic composites can offer a large profile of mechanical properties, depending on the constitution of the composites and processing conditions during its production. A critical issue in the processing of semicrystalline thermoplastic composites is the morphology in the matrix and at the fiber/matrix interface. Both of them have a profound effect on the ultimate properties of the composites.

Transcrystallization is an oriented crystallization found at the fiber/matrix interface in some semicrystalline thermoplastic composites. It develops in the form of a column around the fiber. Its lamellae grow perpendicular to the fiber. Although this unique interface morphology has been reported to improve the mechanical properties of some fiber-reinforced composites,[1,2] the mechanism of transcrystallization has not been fully understood. In particular, there have not been any rules on which the appearance of transcrystallization in a fiber/matrix system can be predicted accurately. Many factors, such as fiber topography, surface coating on the fiber, and processing conditions of the composites, have been reported to influence the nucleation of transcrystallization to some extent.[1–9]

Temperature gradients have been used for the investigation of polymer crystallization for many years.[10–14] Since the temperature dependence of nucleation rate and lamellae growth rate can be visualized by crystallizing one sample in a temperature gradient, it should be necessary to find its application to the investigation of transcrystallization. This article relates the transcrystalliza-

Correspondence to: J. Petermann.

Table I Matrix and Fibers

Matrix or Fiber		Type	Manufacturer
Matrix	iPP	B1685/Z1, Granular (T_m = 175°C, MFI = 2.5)	BASF, Germany
Fiber	Carbon fiber		
	UHM	FT700 (based on pitch, no sizing)	Tonen, Japan
	HM	FT500 (based on pitch, no sizing)	Tonen, Japan
	IM	T800 (based on PAN, no sizing)	Toray, Japan
	HT	T300 (based on PAN, with sizing)	Soficar, France
	Aramid fiber		
	Twaron	D1056	AKZO, the Netherlands
	GF	RO99 1200 P139	Vetrotex, Germany

tion of fiber-reinforced isotactic polypropylene (iPP) composites in a temperature gradient. The mechanism of the transcrystallization is discussed with a combination of the new results and some results published in the literature.

EXPERIMENTAL

Materials

In this work, one iPP matrix and six different fibers were used. They are listed in Table I. All of these fibers were used as supplied from the manufacturers. No further surface treatment was made.

Temperature Gradient Apparatus

Figure 1 is the scheme of the temperature gradient apparatus used in this work. It consists mainly of two copper blocks controlled to be of different temperatures with heating elements and thermocouples. The distance between the two blocks is 4.5 mm. A temperature gradient exists between the two blocks. The actual temperature distribution of the temperature gradient was calibrated using the melting points of phenacetin (T_m = 134.5°C), benzanilid (T_m = 163°C), and saluphen (T_m = 191°C) (Fig. 2). For fiber pulling, a fine pulling machine was mounted on a side of the temperature gradient apparatus. The temperature gradient apparatus was installed under a polarizing light microscope for the observation of the crystallization process *in situ*.

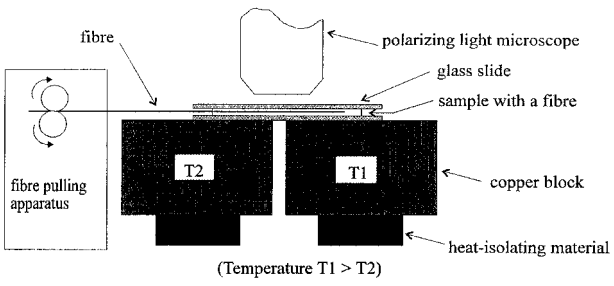

Figure 1 Scheme of the temperature gradient apparatus.

Sample Preparation and Experimental Procedures

A small piece (10 × 10 × 0.05 mm) of polypropylene film (previously compression molded between two glass plates) was placed on a microscope slide being held at 196°C on the hotter block (T1) of the temperature gradient apparatus. A single fiber was set on the molten polypropylene film and

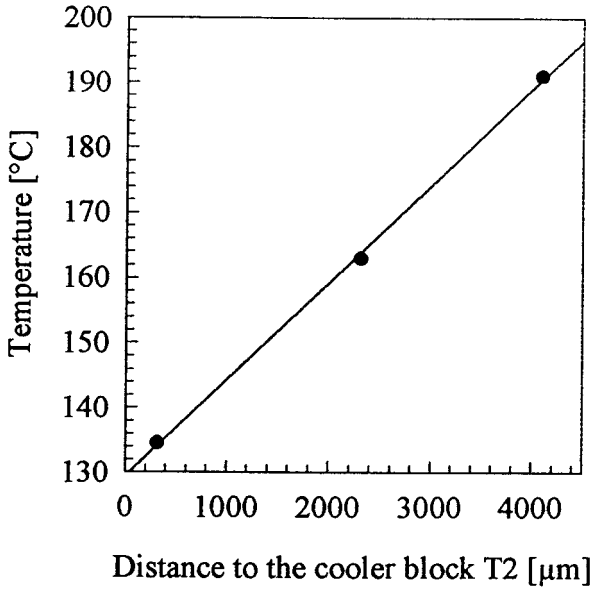

Figure 2 Temperature distribution in the temperature gradient.

covered by another piece of the polypropylene film and a cover slip. The sandwich was kept at 196°C for 5 min and then quickly moved onto the temperature gradient. If necessary, the fiber was then pulled for 10 sec and stopped. A polarizing light microscope (Olympus CH-2) with a photo camera was used to observe the crystallization process *in situ*.

A scanning electron microscope (Hitachi S-4500) was used to investigate the fiber surfaces. Since a low acceleration voltage (1 KV) was used, it was not necessary to coat the samples with any metals.

RESULTS AND DISCUSSION

Nucleation Abilities of the Fibers in iPP

Figure 3 shows polarized light micrographs indicating the crystallization of iPP on the fibers in the temperature gradient. It is shown that these fibers have different nucleation abilities in the iPP matrix at certain temperatures. The Ultra-High-Module carbon fiber (UHMCF), the High-Module carbon fiber (HMCF), and Twaron have good nucleation ability and have induced the transcrystallization of iPP in certain temperature ranges. The nucleation abilities of the three fibers are, however, not identical. Among them, UHMCF indicated the best nucleation ability in iPP. Intermediate-Module carbon fiber (IMCF), High-Tenacity carbon fiber (HTCF), and E-glass fiber (GF) showed no good nucleation ability in iPP. No transcrystallization happened on their surfaces.

With the increase of the crystallization temperature from about 132 to 146°C, the nucleation density of iPP transcrystallization on the fiber surfaces decreases. Continuous nucleation can be seen only to 145°C on UHMCF, 143°C on HMCF, and 137°C on Twaron within the crystallization period of 30 min. This means that there is an upper temperature limit for every fiber, above which the nuclei density on the fiber surface is too rare to form transcrystallization. At the same time, the nuclei density in the matrix also decreased with the increase of the crystallization temperature. At the other side, the transcrystallite length (perpendicular to the fiber) depended strongly on the temperature. It became shorter with increasing temperatures. From Figure 3, one can see the advantage of applying temperature gradients in the investigation of transcrystallization in fiber-reinforced thermoplastic composites: it is the simple visualization of the temperature dependence of nucleation and the lamellae growth of transcrystallites in a single experiment.

Fiber Surface Topography

In order to survey the influence of the fiber surface topography on transcrystallization, scanning electron microscopy of the fiber surface was made (Fig. 4). From Figure 4, one can observe the fiber surface situations. The pitch-based carbon fibers (UHMCF and HMCF) have quite different surface topography, when being compared with the PAN-based carbon fibers (IMCF and HTCF). The surfaces of pitch-based carbon fibers are much rougher. There exist numerous edge planes of graphite layers, which are ordered parallel to the fiber axis. In the case of PAN-based carbon fibers, the surfaces are not so rough and the edge planes are not so densely located as on the pitch-based ones. In comparison to carbon fibers, the glass fiber and Twaron have quite smooth surfaces. Only some sizing particles can be observed on their surfaces.

Shear-Induced Transcrystallization

Shear was applied to the fiber/matrix interface by pulling the fiber in the matrix melt before the beginning of the crystallization. Figures 5 and 6 show the shear-induced transcrystallization in the temperature gradient.

Figure 5 indicates that IMCF, HTCF, and GF, which did not induce the transcrystallization of iPP in quiescent conditions (Fig. 3), have succeeded in inducing transcrystallization after the fibers were pulled. Here, it is called shear-induced transcrystallization. The temperature dependence of nucleation density and of transcrystallite growth appears to be similar to that of the transcrystallization conducted in quiescent conditions [Fig. 3(a–c)]. The similarity is that the nuclei density and the transcrystallite length are decreasing with increasing temperatures. Comparing Figure 5(b) and Figure 6, one can find out the difference between the shear-induced transcrystallization and the transcrystallization conducted in quiescent conditions: the nuclei density of the shear-induced transcrystallization depends not only on the crystallization temperature but also on the pulling rate of the fiber. Raising the fiber

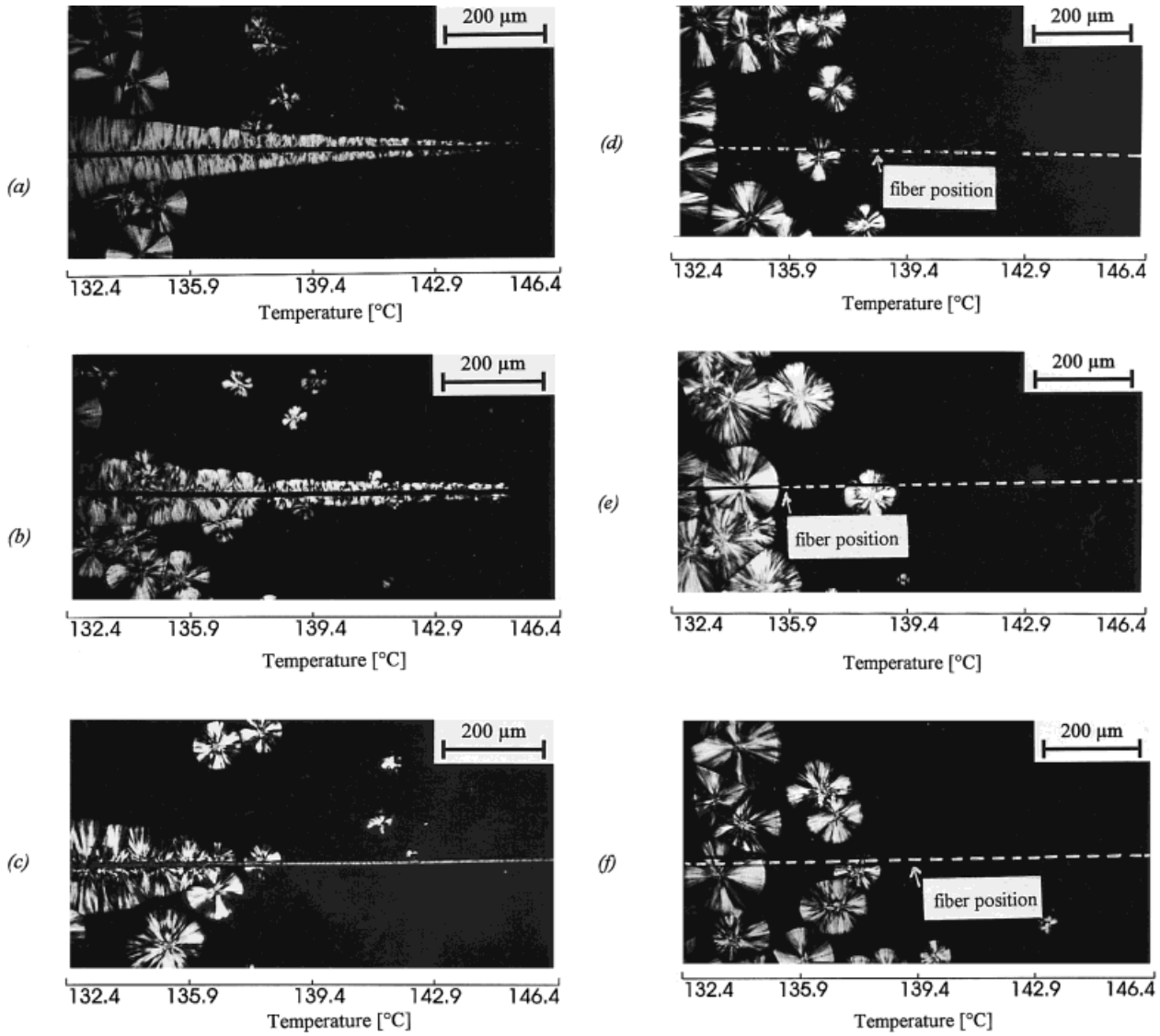

Figure 3 Polarized light micrographs indicating the crystallization of iPP on the fibers in the temperature gradient: (a) UHMCF/iPP, (b) HMCF/iPP, (c) Twaron/iPP, (d) IMCF/iPP, (e) HTCF/iPP, and (f) GF/iPP; crystallization time, t_c = 30 min.

pulling rate leads to an increase of nuclei density on the fiber at the same temperature. In other words, the increase of the fiber pulling rate causes the increase of the upper temperature limit, above which the nuclei on the fiber surface are too rare to form the transcrystallites.

The crystallographic form of iPP transcrystallites, shown in Figures 3, 5, and 6, is identical to that of iPP spherulites in the bulk. It is α-form iPP.

The dependence of iPP transcrystallization on fiber types has been already investigated in isothermal crystallization conditions.[8,15,16] Their results have indicated that HMCF and Twaron tend to induce transcrystallization; it is difficult to induce transcrystallization with other carbon fibers and GF without pulling the fibers in the matrix melt. These are well in accordance with the results shown in Figures 3 and 5. However, the difference between the nucleation ability of HMCF and Twaron, which is shown in Figure 3, has rarely been investigated. Therefore, it is necessary to combine the new results out of this work with the results published earlier to get a deeper understanding of the mechanism of transcrystallization.

The nucleation of the transcrystalline growth is very specific to fiber/matrix combinations. The following factors have been considered to influence the nucleation of transcrystallization[17]:

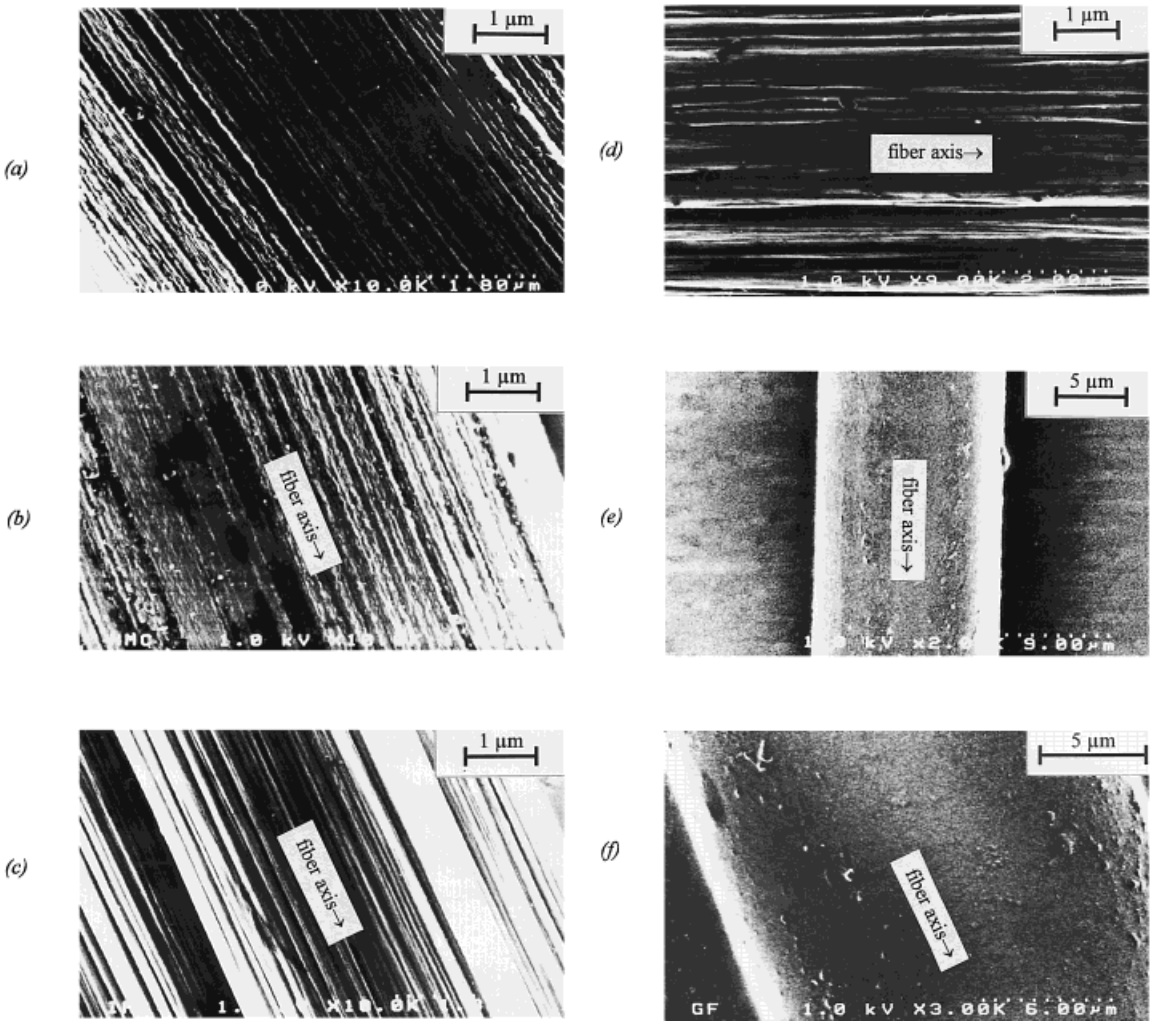

Figure 4 Scanning electron micrographs showing fiber surface topography: (a) UHMCF, (b) HMCF, (c) IMCF, (d) HTCF, (e) Twaron, and (f) GF.

- epitaxy between the fiber and matrix,
- topography of the fiber,
- mismatch of thermal expansion coefficients between the fiber and matrix,
- thermal conductivity of the fiber,
- chemical composition of the fiber surface, and
- surface energy of the fiber.

However, it has not been determined which mechanism is comprehensively valid to the transcrystallization in most fiber/matrix systems.

Fiber topography was used to explain the different nucleation abilities of pitch-based HMCF and PAN-based carbon fibers in thermoplastic matrices.[17,18] According to this explanation, the numerous edge planes of graphite on the pitch-based HMCF [Fig. 4(a,b)] can cause epitaxy effects between the fiber and matrix, leading to the nucleation of transcrystallization. The PAN-based carbon fibers permit no accommodation of nuclei on their surfaces since they contain mostly defect-free basal planes on their surfaces.[18,19] This explanation cannot, however, be applied to interpret the transcrystallization on the surfaces of glass fibers and Twaron, because there are no edge planes, not even crystalline textures on glass fibers.

Thomason and Van Rooyen[15] tried to explain transcrystallization with shear-induced crystallization at the fiber/matrix interface. According to that, transcrystallization should be induced by the interface shear arising from the different extents of linear shrinkage of fiber and matrix during the cooling process. This theory seems to be valid, as shown by the results in Figures 3 and 5. The mismatch of

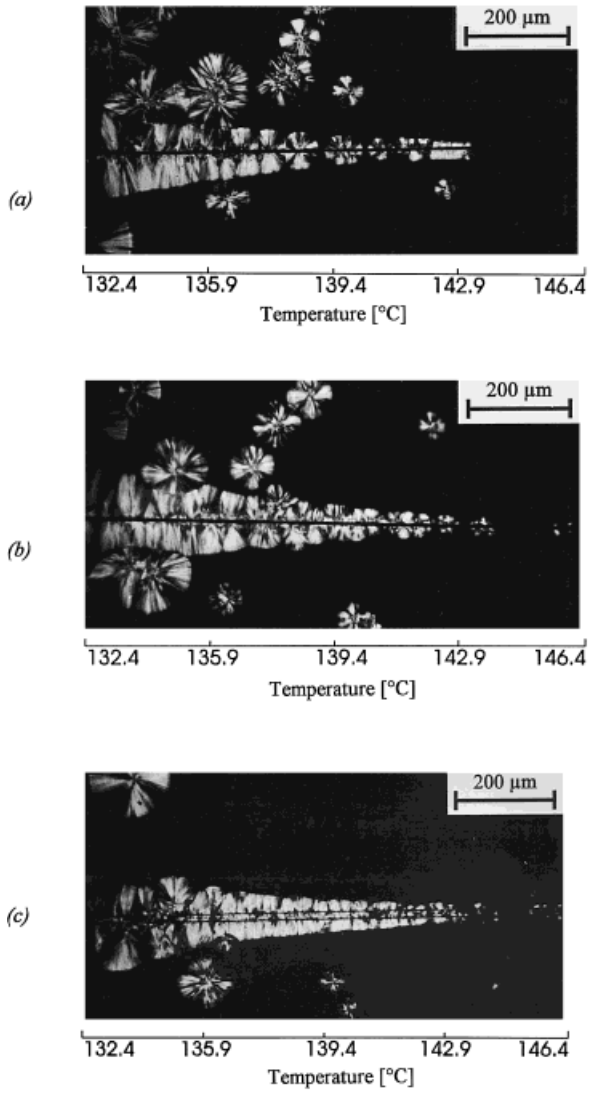

Figure 5 Polarized light micrographs showing shear-induced transcrystallization around (a) IMCF, (b) HTCF, and (c) GF. Fiber pulling rate, γ = 0.54 mm/min; crystallization time, t_c = 30 min.

thermal expansion coefficients (α-mismatch) between the fibers and the matrix used in this experiment (Table II) is in the order UHMCF/iPP > HMCF/iPP > IMCF/iPP or HTCF/iPP.

The interface shear resulting from α-mismatch on the cooling of the composites should be in the same order. Therefore, UHMCF and HMCF can induce transcrystallization because of the large α-mismatch to the matrix, while IMCF and HTCF cannot, because of small α-mismatch to the matrix. Among them, UHMCF showed the best nucleation ability, since the interface shear is the largest.

Twaron has larger α-mismatch than UHMCF and HMCF. However, it showed lower nucleation ability, when compared with UHMCF and HMCF at the same temperatures [Fig. 3(a–c)]. This cannot be interpreted only with the theory suggested by Thomason and Rooyen.

Table II Thermal Expansion Coefficient (α) of iPP Melt and Fibers

Melt or Fiber	$\alpha[10^{-6}\ °C^{-1}]$
iPP melt	+300[15]
UHM-CF (parallel to fiber axis)	−1.5[a]
HM-CF (parallel to fiber axis)	−1.0[a]
IM-CF (parallel to fiber axis)	−0.1 to −0.5[20]
HT-CF (parallel to fiber axis)	−0.1 to −0.5[20]
GF	+4.9[20]
Twaron (parallel to fiber axis)	−3.5[15]

[a] Supplied by fiber producers.

The temperature gradient at the fiber/matrix interface caused by the mismatch of the thermal conductivity between fiber and matrix (λ-mismatch) on sample cooling for crystallization could be another possible reason for transcrystallization. This suggestion is verified by the oriented crystallization of polybutene-1[14] and iPP[21] in a temperature gradient. The nature of the lamellae orientation in a temperature gradient appears to be identical to that of the transcrystallization under isothermal conditions.[21] It is well known that the fibers normally have better thermal conductivity (λ) than the matrix (Table III). If a fiber/matrix system is cooled from a high temperature (normally, above the melt temperature of the matrix) to a crystallization temperature, the fiber reaches the crystallization temperature earlier than the matrix because of the faster heat trans-

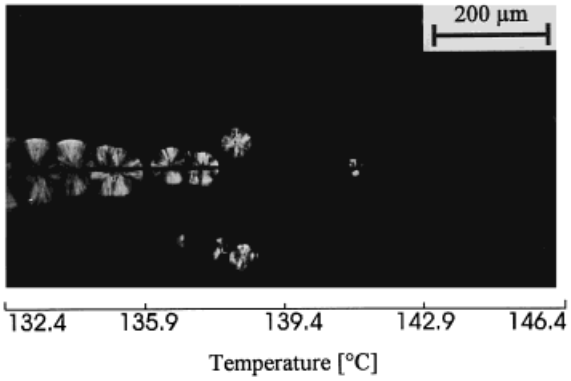

Figure 6 Polarized light micrographs showing shear-induced transcrystallization around HTCF. Fiber pulling rate γ = 0.27 mm/min.

Table III Thermal Conductivity (λ) of Matrix and Fibers

Matrix or Fiber	λ [W m^{-1} $°C^{-1}$]
iPP matrix	0.20[20]
UHM-CF (parallel to fiber axis)	360[a]
HM-CF (parallel to fiber axis)	150[a]
IM-CF (parallel to fiber axis)	24[20]
HT-CF (parallel to fiber axis)	24[20]
GF	1.04[20]
Twaron (parallel to fiber axis)	0.04[20]

[a] Supplied by fiber producers.

port of the fiber. This will lead to a temperature gradient at the fiber/matrix interface, where the matrix on the fiber surface has a lower temperature than the matrix far away from the fiber. If the temperature gradient is quite large, the nucleation should happen at first on the fiber surface. The simultaneous growth of numerous nuclei from the fiber surface and the steric hindrance in all directions except the direction perpendicular to the fiber make the lamellae grow perpendicular to the fiber. This causes the formation of transcrystallization around the fiber.

On the other hand, the lower matrix temperature near the fiber leads to the increase of the matrix melt viscosity and consequently the increase of the interface shear on sample cooling. Therefore, in addition to α-mismatch, λ-mismatch may also play an important role in the induction of the transcrystallization.

With the combination of the two factors, α-mismatch and λ-mismatch, one can suggest a reasonable explanation for the results obtained in this work: UHMCF and HMCF have both a large α-mismatch (Table II) and a large λ-mismatch (Table III) to the iPP matrix. The interface shear and interface temperature gradient on sample cooling for crystallization are supposed to be larger than that of other fibers. Therefore, they can induce transcrystallization easily. Since the IMCF, HTCF, and GF have neither large enough α-mismatch nor large enough λ-mismatch to the iPP matrix, the interface shear and interface temperature gradient cannot be large enough to induce the transcrystallization. In the case of Twaron, the large α-mismatch can lead to a large interface shear rate, but the small λ-mismatch barely causes an interface temperature gradient. The interface shear cannot be as large as in the case of UHMCF and HMCF. Its nucleation ability to the iPP matrix is therefore not as good as that of UHMCF and HMCF, which is shown in Figure 3.

Regarding the discussion above, one can put forth a comprehensively valid mechanism of transcrystallization (Fig. 7). According to this mechanism, transcrystallization should be mainly induced by two factors: fiber/matrix interface shear and interface temperature gradient arising on sample cooling for crystallization. Transcrystallization can be induced if either of them appears to be quite large. Many other factors, such as the sample cooling rate for the crystallization, fiber topography, fiber/matrix adhesion or wettability, matrix molecular weight, and chemical composition of the matrix, have certain effects on the creation of the fiber/matrix interface shear and interface temperature gradient. Therefore, they are also related to the transcrystallization.

The mechanism of transcrystallization in Figure 7 seems to be explained by the theory on heterogeneous nucleation by Binsbergen.[22] He carried out a large amount of research work on the nucleating activity of many different nucleating materials for the crystallization of polyolefins and concluded that the nucleating activity of nucleating agents is not based on their high surface free energy or on epitaxy. It is the prealignment of polymer chains arising from a high degree of accommodation of polymer molecules at the surface of the nucleating agents that facilitates the crystallization. The influence of the prealignment or orientation of polymer chains to crystallization kinetics was intensively investigated by Ziabicki.[23]

In the case of transcrystallization in fiber-reinforced thermoplastic composites, the fiber is the nucleating agent. The fiber/matrix interface shear causes prealignment of matrix molecule chains in the longitudinal direction of the fiber and thus facilitates the crystallization on the fiber surface. The fiber/matrix interface temperature gradient enhances the formation of the transcrystallization because of a larger degree of supercooling for the crystallization. A better understanding can be reached with the mechanism shown in Figure 7. A few examples are given below.

1. As is commonly reported, the transcrystallization of iPP on GF is difficult to induce under normal crystallization conditions. However, Thomason and Van Rooyen[15] have succeeded in inducing the transcrystallization of iPP on GF, using a large cooling rate (280°C/min) for the crystallization. This phenomenon can be easily inter-

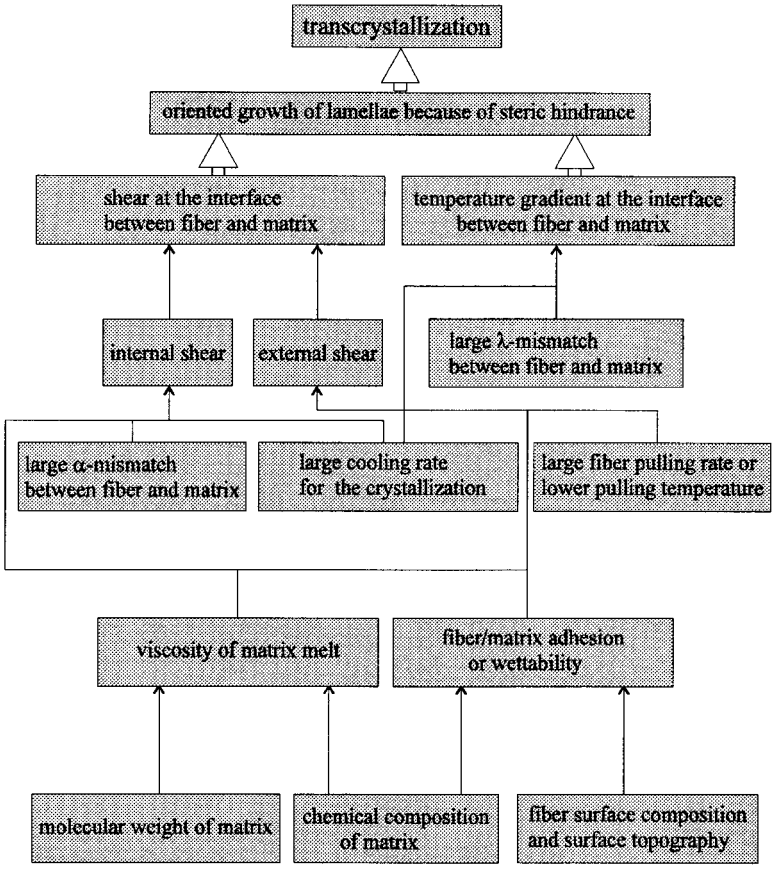

Figure 7 Mechanism of transcrystallization.

preted by means of the mechanism shown in Figure 7: although the α-mismatch and the λ-mismatch of GF/iPP system are not large, such a fast cooling rate can cause quite a large interface shear and interface temperature gradient, leading to the formation of transcrystallization. This example indicates the importance of the cooling rate in the transcrystallization.

2. As shown in Figure 3(d,e), PAN-based IMCF and HTCF have bad nucleation ability to the iPP matrix. Without the application of external shear (by fiber pulling), no transcrystallization normally happens on these fibers. However, one cannot draw the conclusion that these fibers have bad nucleation ability in all semicrystalline thermoplastic matrices, because the chemical composition of the matrix and the adhesion or wettability between fiber and matrix also have an influence on the induction of transcrystallization. For example, Nylon 6 molecules have polar chemical groups (—CO— and —NH—). Its adhesion or wettability to GF is much better than to iPP. The fiber/matrix interface shear on the sample cooling should be larger in a GF/Nylon 6 system than in a GF/iPP system. Therefore, it should be easier to induce transcrystallization of Nylon 6 on GF under normal crystallization conditions. In fact, this was already verified in the research work of Bessel and Shortall.[24]
3. Fiber topography and fiber surface sizing influence the fiber/matrix adhesion and also have an effect on transcrystallization. One convincing example is that natural cellulose fibers can induce the transcrystallization of iPP,[25] while the same fibers surface treated cannot,[26] although the crystallization condition remains the same.

CONCLUSIONS

By investigation of the transcrystallization of iPP on UHMCF, HMCF, IMCF, HTCF, GF, and

Twaron in a temperature gradient, the different nucleation abilities of these fibers to the matrix iPP were visualized by means of a polarizing microscope. A new suggestion as to the mechanism of the transcrystallization was made. The fiber/matrix interface shear and interface temperature gradient arising on sample cooling for crystallization are supposed to be two important factors leading to the transcrystallization. However, these factors were only discussed qualitatively. In future work, a quantitative estimation of the interface shear and interface temperature gradient should be made under isothermal conditions.

The authors acknowledge the financial support of the Chinese Education Ministry and German Max Buchner-Forschungsstiftung. They express their sincere thanks to Prof. K. Schulte (Technical University of Hamburg-Harburg, Germany) and BASF for supplying fibers and matrix.

REFERENCES

1. R. H. Burton and M. J. Folkes, *Plast. Rubb. Proc. Appl.,* **3,** 129 (1983).
2. J. A. Peacock, B. Fife, E. Nield, and C. Y. Barlow, in *Composite Interfaces,* H. Ishida and J. L. Koenig, Eds., Elsevier, New York, 1986, p. 143.
3. D. G. Gray, *J. Polym. Sci. Polym. Lett. Ed.,* **12,** 645 (1974).
4. D. Campbell and M. M. Qayyum, *J. Mater. Sci.,* **12,** 2427 (1977).
5. M. G. Huson and W. J. Mcgill, *J. Polym. Sci. Polym. Phys. Ed.,* **23,** 121 (1985).
6. E. Devaux and B. Chabert, *Polym. Comm.,* **32,** 464 (1991).
7. E. J. H. Chen and B. S. Hsiao, *Polym. Eng. Sci.,* **32**(4), 280 (1992).
8. J. L. Thomason and A. A. Van Rooyen, *J. Mater. Sci.,* **27,** 889 (1992).
9. H. Janeschitz-Kriegel, *Progr. Colloid Polym. Sci.,* **87,** 117 (1992).
10. K. Sasaguri and R. Yamada, *J. Appl. Phys.,* **35,** 3188 (1964).
11. J. M. Crissman and E. Passaglia, *J. Res. Nat. Bur. Std.,* **70A,** 225 (1966).
12. A. J. Lovinger, *J. Appl. Phys.,* **49,** 5003 (1978).
13. A. J. Lovinger and C. C. Gryte, *Macromolecules,* **9,** 247 (1976).
14. Y. Huang and J. Petermann, *Polym. Bull.,* **24,** 649 (1990).
15. J. L. Thomason and A. A. Van Rooyen, *J. Mater. Sci.,* **27,** 897 (1992).
16. J. Varga and J. Karger-Kocsis, *Polym. Bull.,* **30,** 105 (1993).
17. M. J. Folkes, in *Polypropylene: Structure, Blends and Composites,* J. Karga-Kocsis, Ed., Chapman & Hall, London, 1994, Chap. 3.10, p. 13.
18. S. Y. Hobbs, *Nat. Phys. Sci.,* **12,** 234 (1971).
19. A. Oberlin, *Carbon,* **22,** 521 (1984).
20. D. Hull, in *An Introduction to Composite Materials,* D. Hull, Ed., Cambridge University Press, Cambridge, 1981, p. 14.
21. Y. Cai, J. Petermann, and H. Wittich, *J. Mater. Sci. Lett.,* **14,** 1773 (1995).
22. F. L. Binsbergen, *J. Polym. Sci. Polym. Phys. Ed.,* **11,** 117 (1973).
23. A. Ziabicki, *Colloid Polym. Sci.,* **252,** 207 (1974).
24. T. Bessel and J. B. Shortall, *J. Mater. Sci.,* **10,** 2035 (1975).
25. D. G. Gray, *J. Polym. Sci., Polym. Lett. Ed.,* **12,** 509 (1974).
26. D. T. Quilin, D. F. Caulfield, and J. A. Koutsky, *J. Appl. Polym. Sci.,* **50,** 1187 (1993).